

Synthesis and Structural Characterization of Sodalites with Acetate and Formate Guest Anions, $[\text{Na}_4(\text{CH}_3\text{COO})]_2[\text{Al}_3\text{Si}_3\text{O}_{12}]_2$ and $[\text{Na}_4(\text{HCOO})]_2[\text{Al}_3\text{Si}_3\text{O}_{12}]_2$, and Their Intracage Oxidation Product $[\text{Na}_5(\text{CO}_3)][\text{Na}_3\Box][\text{Al}_3\text{Si}_3\text{O}_{12}]_2^1$

Peter Sieger,* Andreas M. Schneider, Michael Wiebcke, Peter Behrens, and Jürgen Felsche

Fakultät für Chemie, Universität Konstanz, Postfach 5560, 78434 Konstanz, Germany

Günter Engelhardt

Institut für Technische Chemie I, Universität Stuttgart,
Pfaffenwaldring 55, 70550 Stuttgart, Germany

Received July 22, 1994. Revised Manuscript Received September 14, 1994[®]

Single-crystals of sodium acetate sodalite $[\text{Na}_4(\text{CH}_3\text{COO})]_2[\text{Al}_3\text{Si}_3\text{O}_{12}]_2$ (**1**) and polycrystalline material of sodium formate sodalite $[\text{Na}_4(\text{HCOO})]_2[\text{Al}_3\text{Si}_3\text{O}_{12}]_2$ (**2**) were synthesized under hydrothermal conditions. The interactions between the organic anions, Na cations, and the aluminosilicate sodalite framework, as well as the intracage reactivity of the enclathrated anions versus oxidation were investigated. Therefore, the crystal structures of **1** and **2** were refined based on single-crystal and powder X-ray diffraction data, respectively. Additionally, the compounds were characterized by thermoanalytical methods as well as infrared and multinuclear MAS NMR spectroscopy. **1** and **2** crystallize with the cubic space group $P43n$ ($Z = 1$) and the cell constants (room temperature) $a = 9.077(2)$ Å and $a = 8.960(2)$ Å, respectively. The 1:1 aluminosilicate host framework of **1** and **2** is a strictly alternating array of corner-linked AlO_4 and SiO_4 tetrahedra. Each $[4^66^8]$ polyhedral void is occupied by four Na^+ cations, located close to oxygen atoms of the six-membered rings of the frameworks, and by one organic anion (CH_3COO^- or HCOO^-) at the center. When **1** and **2** are annealed in air or oxygen at 1123 K and 923 K, respectively, intracage oxidation of the anion takes place without decomposition of the host framework, resulting in both cases in the same new sodalite phase which contains carbonate anions as a guest species. Sodium carbonate sodalite, $[\text{Na}_5(\text{CO}_3)][\text{Na}_3\Box][\text{Al}_3\text{Si}_3\text{O}_{12}]_2$ (**3**), is cubic with the cell constant $a = 9.040(3)$ Å (room temperature) and the space group $P23$ ($Z = 1$). A Rietveld refinement based on powder X-ray diffraction data revealed that the sodalite cages of **3** are filled alternatively with $[\text{Na}_5(\text{CO}_3)]$ and $[\text{Na}_3\Box]$ complexes in an ordered manner.

Introduction

Sodalites are host-guest compounds with a three-dimensional four-connected framework built up from corner-sharing TX_4 tetrahedra. Meanwhile, sodalites have been synthesized with a vast number of element combinations in the TX_4 units (e.g., T = Be, Zn, B, Al, Ga, Si, Ge, P, As, and X = O; T = P and X = N).² In the host framework, which is based on the space-filling $[4^66^8]$ truncated octahedron (also known as sodalite cage or β -cage), a large variety of cationic, anionic, and/or neutral guest species can be enclathrated. Depending on the composition, sodalites possess photochromic,

cathodochromic, or ion-conducting properties,³ and show redox or decomposition reactions inside their β -cages ("intracage chemistry").⁴ Especially, a Ag-exchanged sodalite containing organic oxalate anions was shown to exhibit an intriguing photochromic behavior which was related to a photochemically induced redox reaction.⁵ These materials have very recently also attracted considerable attention as matrices for metal and semiconductor clusters and extended superclusters in the quantum size regime ("nanocomposites").⁶

* Author for correspondence. Present address: Department of Chemistry, University of California, Santa Barbara, CA 93106.

[®] Abstract published in *Advance ACS Abstracts*, October 15, 1994.

(1) In a brief form already presented by the same authors at the Fifth German Workshop on Zeolite Chemistry, Leipzig, March 1993.

(2) Depmeier, W. *Acta Crystallogr.* **1984**, *B40*, 185. Gier, T. E.; Harrison, W. T. A.; Stucky, G. D. *Angew. Chem.* **1991**, *103*, 1191; *Angew. Chem., Int. Ed. Engl.* **1991**, *30*, 1169. Nenoff, T. M.; Harrison, W. T. A.; Gier, T. E.; Stucky, G. D. *J. Am. Chem. Soc.* **1991**, *113*, 378. Sokolova, E. V.; Rybakov, V. B.; Patov, L. A. *Sov. Phys. Dokl.* **1991**, *36*, 276. Schnick, W.; Lücke, J. *Angew. Chem.* **1992**, *104*, 208. *Angew. Chem., Int. Ed. Engl.* **1992**, *31*, 213.

(3) Van Doorn, C. Z.; Schipper, D. J.; Bolwijn, P. T. *J. Electrochem. Soc.* **1972**, *119*, 85; *J. Appl. Phys.* **1972**, *43*, 132. Taylor, M.; Marshall, D. J.; Evans, H. *J. Phys. Chem. Solids* **1971**, *32*, 2021; Takeda, T.; Watanabe, A. *J. Electrochem. Soc.* **1973**, *120*, 114.

(4) Weller, M. T.; Wong, G.; Adamson, C. L.; Dodd, S. M.; Roe, J. J. *B. J. Chem. Soc., Dalton Trans.* **1990**, 593. Weller, M. T.; Haworth, K. E. *J. Chem. Soc., Chem. Commun.* **1991**, 734. Buhl, J.-Ch. *J. Solid State Chem.* **1991**, *94*, 19.

(5) Stein, A.; Ozin, G. A.; Stucky, G. D.; *J. Soc. Photogr. Sci. Technol. Jpn.* **1990**, *53*, 322.

(6) Ozin, G. A.; Kuperman, A.; Stein, A. *Angew. Chem., Adv. Mater.* **1989**, *101*, 373. Stucky, G. D.; McDougall, J. E. *Science* **1990**, *247*, 669. Ozin, G. A.; Kirkby, S.; Meszaros, M.; Ozkar, S.; Stein, A.; Stucky, G. D. *ACS Symp. Ser.* **1991**, *455*, 554. Stein, A.; Ozin, G. A.; Stucky, G. D. *J. Am. Chem. Soc.* **1992**, *114*, 8119.

Since the sodalite cage is a polyhedral building unit of some industrially important zeolites (e.g., zeolite A, cubic, and hexagonal faujasite⁷), sodalite compounds have been considered as a model system for studying pure β -cage properties.⁸ Studies on sodalites containing organic anions should provide important insight with regard to weak and strong, attractive and repulsive, interactions between organic molecules and inorganic solid matter. These features, found in a system with model character, also have implications on the interaction of organic molecules with inorganic solid matter in other fields such as heterogeneous catalysis, biomineralization, and biomimetic synthesis procedures.

Therefore, a detailed understanding of the guest–host as well as guest–guest interactions is of fundamental importance. A particular aim of our studies on sodalites is to gain deeper insight into these interactions, which are ionic and van der Waals forces as well as hydrogen bonds and determine the orientations and dynamics of the guest species. In contrast to other clathrates, the high thermal stability of the aluminosilicate sodalite host framework helps us to investigate the dynamical behavior of “matrix isolated” guest complexes over a wide range of correlation times. Recently, we have reported the results of our studies on the aluminosilicate sodalites $[\text{Na}_4(\text{H}_3\text{O}_2)_2][\text{Al}_3\text{Si}_3\text{O}_{12}]_2$, $[\text{Na}_4(\text{OH})_2][\text{Al}_3\text{Si}_3\text{O}_{12}]_2$, and $[\text{Na}_3\Box(\text{H}_2\text{O})_4][\text{Al}_3\text{Si}_3\text{O}_{12}]_2$ (\Box denotes a vacancy in a Na_4 tetrahedron)⁹ and $[\text{Na}_4(\text{B}(\text{OH})_4)_2][\text{Al}_3\text{Si}_3\text{O}_{12}]_2$.¹⁰ Also, materials with only one kind of tetrahedral framework atom such as silica sodalites $[\text{M}]_2[\text{Si}_6\text{O}_{12}]_2$ (with M = ethylene glycol, trioxane, dioxolane, ethylenediamine, ethanolamine)¹¹ and aluminate sodalites $[\text{M}_4(\text{XO}_4)_2][\text{Al}_6\text{O}_{12}]_2$ (with M = Ca, Sr and X = S, Cr, Mo, W)¹² are currently under investigation.

Here, we report on the hydrothermal synthesis of the sodalites **1** and **2** and on their intracage oxidation to yield the sodalite **3**. The materials were characterized by single-crystal and powder X-ray diffraction as well as thermoanalytical methods and infrared and MAS NMR spectroscopy.

Experimental Section

Preparation. Single crystals of **1** were synthesized hydrothermally. The reaction mixtures were sealed in silver tubes of 8 mm diameter and 100 mm lengths packed in high-pressure steel autoclaves. A typical reaction mixture contained 200 mg of kaolinite (Fluka), which had been sintered at 1773 K, and 320 mg of anhydrous sodium acetate (Merck) and 2 mL of carbonate-free 8 M NaOH (Riedel-de-Haen) (molar ratios: $\text{Al}_4\text{Si}_4\text{O}_{14} \cdot 8\text{NaH}_3\text{CCOO} : 16\text{NaOH} : \text{aq}$). The autoclaves

Table 1. Experimental Conditions of the MAS NMR Measurements

	¹ H	¹³ C	²³ Na	²⁹ Si
resonance freq (MHz)	400.13	100.63	105.48	79.49
pulse repetition (s)	2	20	5	5
pulse width (μs)	2	2.3	0.7	2
spinning speed (kHz)	10.0	4.5	8.0	4.0
standard	TMS	TMS	NaCl (solid)	TMS

were kept in an oven at 623 K and 110 MPa for 7 days. After cooling to room temperature, the crystals were separated and washed with water until the washing water gave a neutral reaction (pH 7). Finally, the crystals were dried at 373 K for 12 h.

Polycrystalline material of **2** was obtained under mild hydrothermal conditions. Mixtures of 240 mg of SiO_2 (Merck), 204 mg of $\gamma\text{-Al}_2\text{O}_3$ (Merck), 2.72 g of sodium formate (Merck), and 8 mL of carbonate-free 8 M NaOH (molar ratios $2\text{SiO}_2 : \text{Al}_2\text{O}_3 : 20\text{NaHCOO} : 32\text{NaOH} : \text{aq}$) were placed in 10 mL Teflon-coated steel autoclaves and kept at 423 K under autogeneous pressure for 10 days.

Polycrystalline material of **3** was prepared by annealing **1** and **2** in air or oxygen at 1123 K (60 h) and 923 K (16 h), respectively.

Thermal Analysis. Thermogravimetry (TG), derivative thermogravimetry (DTG), and difference thermoanalysis (DTA) were performed simultaneously on a Netzsch thermoanalyzer STA 429 (air or oxygen atmosphere, heating rate 1 and 10 K min^{-1} , Pt crucible, thermocouple Pt10%Rh/Pt). Mass spectrometric analysis was carried out using a Balzers QMG 511 apparatus. Differential scanning calorimetric (DSC) measurements were done on a Perkin-Elmer DSC-7 apparatus using Al containers as sample holders and heating/cooling rates of 10 K min^{-1} .

Spectroscopic Studies. ¹H, ¹³C, ²³Na, and ²⁹Si MAS NMR spectra were recorded on a Bruker MSL-400 spectrometer equipped with double-bearing multinuclear MAS probes for rotors with 4 mm (¹H, ²³Na) and 7 mm diameter (¹³C, ²⁹Si). Single-pulse excitation was applied, for the ¹³C, ²³Na, and ²⁹Si nuclei in combination with high-power proton decoupling. The conditions of the measurements are collected in Table 1.

Mid-IR spectra were recorded on a Mattson-Polaris FTIR spectrometer using KBr pellets of the samples.

X-ray Diffraction Studies. Powder photographs were taken on a Guinier camera (Huber system G 600) with $\text{Cu K}\alpha_1$ radiation (internal standard Si). Unit-cell constants were obtained by LSQS refinement. Details of the single-crystal and powder X-ray diffraction measurements for structure analysis are given in Table 2.

Results and Discussion

The sodalites **1** and **2** have been synthesized hydrothermally by modified procedures derived from the pioneering work of Barrer and co-workers.¹³ Large colorless, transparent crystals of **1** (up to 1.0 mm in size) and polycrystalline material of **2** have been obtained. **3** cannot be prepared directly by similar hydrothermal methods using sodium carbonate instead of the sodium carboxylates. Hydrothermal treatment in the presence of carbonate anions leads to a cancrinite-type material.¹⁴ However, a polycrystalline material of **3** has been obtained by annealing **1** and **2** in flowing air or oxygen at elevated temperatures (see below).

Powder X-ray diffraction photographs identified the materials as pure sodalite phases with a high degree of crystallinity. Differential scanning calorimetric (DSC) measurements on **1**, **2** and **3** revealed that there occur

(7) Meier, W. M.; Olson, D. H. *Atlas of Zeolite Structure Types*, 3rd ed.; Butterworth-Heinemann: London, 1992.

(8) Felsche, J.; Luger, S. *Ber. Bunsen-Ges. Phys. Chem.* **1986**, *90*, 731. Felsche, J.; Luger, S. *Thermochim. Acta* **1987**, *118*, 35.

(9) Luger, S.; Felsche, J.; Fischer, P. *Acta Crystallogr.* **1987**, *C43*, 1; Luger, S.; Felsche, J.; Fischer, P. *Acta Crystallogr.* **1987**, *C43*, 809. Luger, S.; Felsche, J.; Baerlocher, Ch. *Zeolites* **1986**, *6*, 367. Engelhardt, G.; Felsche, J.; Sieger, P. *J. Am. Chem. Soc.* **1992**, *114*, 1173. Elsenhans, O.; Bührer, W.; Anderson, I.; Nicol, J.; Udovic, T.; Rieutord, F.; Felsche, J.; Sieger, P.; Engelhardt, G. *Physica B* **1992**, *180*, 181, 661. Engelhardt, G.; Sieger, P.; Felsche, J. *Angew. Chem.* **1992**, *104*, 1248; *Angew. Chem., Int. Ed. Engl.* **1992**, *31*, 1210.

(10) Buhl, J.-Ch.; Engelhardt, G.; Felsche, J. *Zeolites* **1989**, *9*, 40.

(11) Richardson, J. W.; Pluth, J. J.; Smith, J. V.; Dytrych, W. J.; Bibby, D. M. *J. Phys. Chem.* **1988**, *92*, 243. Keijsper, J.; den Ouden, C. J. *J. Stud. Surf. Sci. Catal.* **1989**, *49A*, 237. van de Goor, G.; Behrens, P.; Felsche, J. *Microporous Mater.* **1994**, *2*, 493.

(12) Depmeier, W. *Phys. Chem. Miner.* **1988**, *15*, 419; Engelhardt, G.; Koller, H.; Sieger, P.; Depmeier, W.; Samoson, A. *Solid State Nucl. Magn. Reson.* **1992**, *1*, 127

(13) Barrer, R. M.; Cole, J. F.; Sticher, H. *J. Chem. Soc.* **1968**, 2475. Barrer, R. M.; Cole, J. F. *J. Chem. Soc.* **1970**, 1516.

(14) Hermeler, G.; Buhl, J.-Ch.; Hoffmann, W. *Acta Crystallogr.* **1990**, *A46*, C-524.

Table 2. Crystal Data and Details of the Measurement of Single-Crystal and Powder X-ray Diffraction Intensities and Structure Refinements for [Na₄(CH₃COO)]₂[Al₃Si₃O₁₂]₂ (1), [Na₄(HCOO)]₂[Al₃Si₃O₁₂]₂ (2), and [Na₅(CO₃)]₂[Al₃Si₃O₁₂]₂ (3)

<i>Crystal data:</i> 1: cubic group $P\bar{4}3n$, $Z = 1$, $a = 9.077(2) \text{ \AA}$, $V = 747.9 \text{ \AA}^3$, $T = 298 \text{ K}$, $d_{\text{calc}} = 2.257 \text{ Mg m}^{-3}$; 2: cubic, space group $P\bar{4}3n$, $Z = 1$, $a = 8.960(2) \text{ \AA}$, $V = 719.3 \text{ \AA}^3$, $T = 298 \text{ K}$, $d_{\text{calc}} = 2.281 \text{ Mg m}^{-3}$; 3: cubic, space group $P23$, $Z = 1$, $a = 9.040(3) \text{ \AA}$, $V = 738.8 \text{ \AA}^3$, $T = 298 \text{ K}$, $d_{\text{calc}} = 2.289 \text{ Mg m}^{-3}$
<i>Single-crystal data collection:</i> 1: rhombic dodecahedral crystal of approximate diameter 0.3 mm, sharp reflections on precession photographs, Enraf-Nonius CAD4 diffractometer, graphite monochromator, Mo $K\alpha$ radiation, $\lambda = 0.71073 \text{ \AA}$, variable $\omega/2\theta$ scan technique, range of indices $0 \leq h, k, l \leq 20$, $2\theta_{\text{max}} = 100^\circ$, a total of 4061 reflections measured, averaging ($R_1 = 0.044$) resulted in 736 unique reflections, reflection conditions were consistent with space group $P\bar{4}3n$, no corrections for absorption ($\mu(\text{Mo } K\alpha) = 0.68 \text{ mm}^{-1}$)
<i>Powder X-ray data collection:</i> Guinier diffraction (Huber G642), asymmetric transmission geometry, Ge monochromator, Cu $K\alpha_1$ radiation, $\lambda = 1.54051 \text{ \AA}$
2: range of measurement $13 \leq 2\theta \leq 100^\circ$, step width $0.02^\circ 2\theta$, 81 contributing reflections
3: range of measurement $7 \leq 2\theta \leq 100^\circ$, step width $0.02^\circ 2\theta$, 158 contributing reflections
<i>Single-crystal refinement:</i> 1: least-squares refinement based on F^2 including all unique reflections, weighting scheme $w = 1/[\sigma^2(F_o^2) + (0.0484P)^2]$ where $P = 1/3[\text{Max}(F_o^2, 0) + 2F_c^2]$, 26 parameters varied in the final cycle, $\Delta/\sigma = 0.00$, wR_2 (on F^2) = 0.079 for all data, R_1 (on F) = 0.028 for 511 reflections with $F_o > 4\sigma(F_o)$, S (on F^2) = 1.075, final difference Fourier synthesis: $\Delta\rho_{\text{max}} = +0.44 \text{ e \AA}^{-3}$ (in 0.5, 0.0, 0.0), $\Delta\rho_{\text{min}} = -0.74 \text{ e \AA}^{-3}$ (in 0.257, x, x)
<i>Powder refinement:</i> Rietveld profile method; 2 [model ii]; 21 parameters varied in final cycle, $\Delta/\sigma < 0.02$, $R_F = 0.092$, $R_{\text{wp}} = 0.152$, $R_{\text{exp}} = 0.100$, $\chi^2 = 2.31$, final difference Fourier synthesis: $\Delta\rho_{\text{max}} = +0.67 \text{ e \AA}^{-3}$ (in 0.25, 0.50, 0.00); 3: 31 parameters varied in final cycle, $\Delta/\sigma < 0.02$, $R_F = 0.092$, $R_{\text{wp}} = 0.118$, $R_{\text{exp}} = 0.092$, $\chi^2 = 3.74$, final difference Fourier synthesis: $\Delta\rho_{\text{max}} = +0.95 \text{ e \AA}^{-3}$ (in 0.18, 0.18, 0.18)
<i>Computer programs:</i> Single-crystal refinement: SHELXL-93 program system ²⁶ with complex atomic scattering factors for neutral atoms as incorporated; ²⁷ powder refinement: XRS82 program package, ²⁸ atomic scattering factors were taken from ref 29

no structural phase transitions in the temperature range 100–400 K. The sodalites have been further characterized by various methods to be described in the following.

Crystal Structure Refinements. Crystal data and details of the measurement of single-crystal (for **1**) and powder X-ray diffraction intensities (for **2** and **3**) are listed in Table 2. The powder data have been analyzed by the Rietveld method.¹⁵ The least-squares refinements for **1**, **2** and **3** started with the coordinates of the host framework atoms Al, Si, and O1 as taken from the literature.¹⁶ The positions of the guest atoms have been determined in subsequent difference Fourier syntheses of the electron density or derived by structure–chemical arguments.

Sodium Acetate Sodalite (1). Two sodium cations, Na1 and Na2, with equal occupancy factor of 0.5, and the carbon atom C of the carboxylate group were localized by difference Fourier methods. Refinements of various models for the orientation of the anion revealed that the carboxylate oxygen and methyl carbon atoms are highly disordered. In particular, the central C–C bond of the anion (m/C_s symmetry) does most probably not coincide with the 2-fold rotation axes of space group $P\bar{4}3n$. In the final refinement the carboxylate oxygen and methyl carbon atom were treated as a single mixed atom X in general position (24i). Hydrogen atoms were not considered. Further details of the structure analysis are collected in Table 2.

Sodium Formate Sodalite (2). By difference Fourier methods only one sodium cation could be localized. Refinement of the framework and Na atoms led to $R_{\text{wp}} = 0.241$. Since the atoms of the formate anion could not be determined, four models were assumed for the

orientational disorder of the anion and refined. In each model the oxygen atoms of the anion were treated as a single atom O2 in general position (24i) of space group $P\bar{4}3n$ and the formyl hydrogen atom was omitted:

- (i) C located in position 2a (0,0,0): center of the cage
- (ii) C located in position 12f ($x, 0, 0$)
- (iii) C located in position 8e (x, x, x ; $x > 0$)
- (iv) C located in position 8e (x, x, x ; $x < 0$)

The refinements of models ii–iv gave comparable R values of $0.077 < R_F < 0.082$ and $0.129 < R_{\text{wp}} < 0.139$, while the refinement of model i resulted in considerably larger R values ($R_F = 0.092$, $R_{\text{wp}} = 0.152$). The final difference Fourier syntheses exhibited maxima of comparable height (0.67 – 0.88 e \AA^{-3} ; in 0.25, 0.5, 0.0). Thus, a distinction between the models ii–iv appears not to be possible on the basis of this Rietveld analysis. However, model ii yields the most reasonable geometrical parameters for the formate anion and has therefore been taken as the best disorder model in the following. Further details of the refinement of model ii are collected in Table 2. The experimental, calculated, and difference powder X-ray diffraction profiles for model ii are shown in Figure 1.

Sodium Carbonate Sodalite (3). Because of the 2-fold negative charge of the carbonate anion, only half of the sodalite cages can be filled with such species. The powder X-ray diffraction pattern (Figure 2) does not exhibit any systematic extinctions as, for example, those characteristic for space group $P\bar{4}3n$. Therefore, space group $P23$ was chosen for structure refinement. This space group, in contrast to space group $P\bar{4}3n$, allows an ordered distribution of the carbonate anions among the β -cages. A difference Fourier synthesis revealed the coordinates of two sodium cations, Na1 and Na2. The carbon atom C of the anion was placed in the center of one of the two crystallographically distinct cages (position 1a), while the oxygen atoms of the anion were treated as a single atom O3 in general position (12j).

(15) Rietveld, H. *Acta Crystallogr.* **1967**, *22*, 151; *J. Appl. Crystallogr.* **1969**, *2*, 65.

(16) Wiebcke, M.; Engelhardt, G.; Felsche, J.; Kempa, P. B.; Sieger, P.; Schefer, J.; Fischer, P. *J. Phys. Chem.* **1992**, *96*, 392.

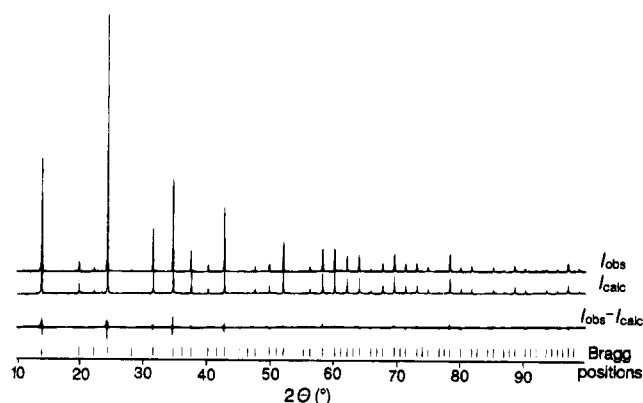


Figure 1. Experimental (I_{obs}), calculated (I_{calc}), and difference ($I_{\text{obs}} - I_{\text{calc}}$) powder X-ray diffraction profiles for $[\text{Na}_4(\text{HCOO})_2][\text{Al}_3\text{Si}_3\text{O}_{12}]_2$ (**2**); the positions of possible Bragg reflections are marked at the bottom.

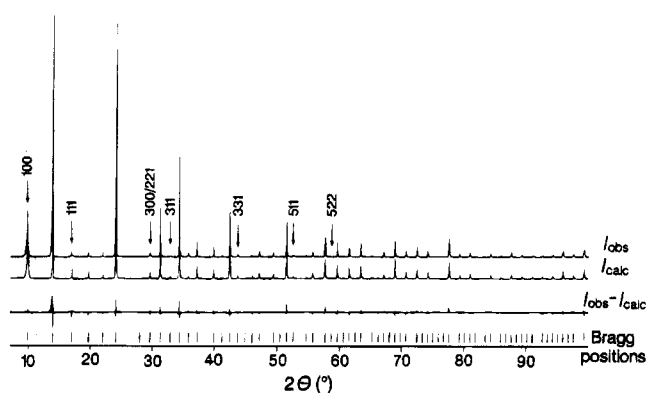


Figure 2. Experimental (I_{obs}), calculated (I_{calc}), and difference ($I_{\text{obs}} - I_{\text{calc}}$) powder X-ray diffraction profiles for $[\text{Na}_5(\text{CO}_3)][\text{Na}_3\Box][\text{Al}_3\text{Si}_3\text{O}_{12}]_2$ (**3**); the positions of possible Bragg reflections are marked at the bottom; arrows indicate peaks that would be absent in the case of space group $P43n$.

Although all atoms had been introduced in the structure model at this stage of the analysis, it was not possible to obtain a good refinement as is indicated by $R_F = 0.149$ and $R_{\text{wp}} = 0.258$. A difference Fourier synthesis exhibited a peak in position $4e(x, x, x; \text{with } x = 0.81)$ which was assigned to a third sodium atom Na3. Only after the Na3 atoms had been taken into account, a satisfactory refinement with considerably improved R values ($R_F = 0.092$ and $R_{\text{wp}} = 0.118$) was obtained. Geometrical constraints for the angle O3-C-O3 (120°) had to be used in the final refinement. Further details of the refinement are collected in Table 2; the structure is discussed later on. The experimental, calculated, and difference powder X-ray diffraction profiles are shown in Figure 2.

General Features of the Crystal Structures of 1–3. The atomic coordinates and displacement parameters obtained by the structure refinements are listed in Tables 3–5 and selected interatomic distances are given in Tables 6–8. The general features of the three-dimensional sodalite framework are discussed in the literature.^{2, 12} The host structures of the compounds under study are strictly alternating arrays of corner-linked AlO_4 and SiO_4 tetrahedra. The high degree of order in the aluminosilicate frameworks is confirmed by the ^{29}Si MAS NMR spectra measured at 298 K, each of which exhibits only one sharp resonance line. The isotropic chemical shift is -89.5 ppm for **1**, -86.7 ppm

for **2**, and -87.9 ppm for **3**. Recently, correlations between ^{29}Si chemical shifts and the cell constants as well as the A–O–Si bond angles have been established for cubic 1:1 aluminosilicate sodalites.¹⁷ Using these correlations, the cell constants and Al–O–Si angles calculated with the ^{29}Si chemical shifts of **1–3** are in good agreement with the corresponding values obtained by the structure analyses.

Structure of Sodium Acetate Sodalite (1). The presence of intact acetate anions is proved by IR spectroscopy. The characteristic $\nu(\text{C-O})$ vibrations are seen at 1420 and 1594 cm^{-1} . The frequencies of the bands deviate slightly from those measured for sodium acetate (1412 and 1575 cm^{-1} ¹⁸). A weak $\nu(\text{C-H})$ band is observed at 3004 cm^{-1} in the IR spectrum of **1**. Thus, the IR spectrum demonstrates that intact acetate anions have been trapped in the sodalite cages during hydrothermal synthesis. In the ^1H MAS NMR spectrum of **1** the methyl protons cause one sharp line at 2.2 ppm (298 K).

Each $[4^68]$ sodalite cage is filled with four sodium cations and one CH_3COO^- anion. The cations are located on the 3-fold axes of the structure in two close, i.e., mutually exclusive, positions Na1 and Na2 ($d(\text{Na1}\cdots\text{Na2}) = 1.328(2)\text{ \AA}$), which are each half-occupied. The highly orientationally disordered anion is located with its carboxylate carbon atom C at the center of the cage. As it was not possible to distinguish between the methyl carbon and the carboxylate oxygen atoms in the structure refinement, these atoms have been modeled by a single mixed atom X in the general position. The polyhedron formed by the X atom around the central C atom on time and space average is shown in Figure 3. The distance C–X at $1.38(2)\text{ \AA}$ is reasonably close to an expected value of 1.33 \AA , calculated as the weighted mean value from the bond lengths C–O (1.25 \AA) and C–C (1.50 \AA) of the anion in crystalline sodium acetate.¹⁹

The orientational disorder of the acetate anion is a consequence of its low symmetry (m/C_s) compared to the high symmetry of the center of the β -cage (23). The simultaneous positional disorder of the sodium cations may be understood, when reference is made to the crystal structure of anhydrous NaCH_3COO .¹⁹ In this orthorhombic structure Na^+ cations are surrounded octahedrally by six oxygen atoms at distances of 2.35 and 2.61 \AA . Layers of such distorted coordination octahedra alternate in the structure with layers containing the methyl groups. Thereby, unfavorable contacts between methyl protons and sodium cations are avoided. In contrast, such a situation cannot be realized within the constraints of a sodalite cage. Here, the sodium cations experience inevitably repulsive Na–H-(anion) or attractive Na–O(anion) interactions, depending on the orientation of the anion. The result is a correlated orientational–positional disorder, with those Na atoms that experience repulsive interactions with the methyl group being modeled by Na2 and those

(17) Engelhardt, G.; Luger, S.; Buhl, J.-Ch.; Felsche, J. *Zeolites* **1989**, *9*, 182. Jacobsen, H. S.; Norby, P.; Bildsoe, H.; Jacobsen, H. J. *Zeolites* **1989**, *9*, 491. Weller, M. T.; Wong, G. J. *Chem. Soc., Chem. Commun.* **1988**, 1103; Newsam, J. M. *J. Phys. Chem.* **1987**, *91*, 1259.

(18) Schrader, B.; Meier, W., Eds., *IR Atlas of Organic Compounds*; Verlag-Chemie: Weinheim, 1977; spectrum B3-17.

(19) Hsu, L.-Y.; Nordman, C. E. *Acta Crystallogr.* **1983**, *C39*, 690.

Table 3. $[\text{Na}_4(\text{CH}_3\text{COO})]_2[\text{Al}_3\text{Si}_3\text{O}_{12}]_2$ (1): Fractional Atomic Coordinates and Displacement Parameters (\AA^2)

atom	Wyckoff position	occupancy factor	x	y	z	U_{iso}^a	atom	U_{11}^a	U_{22}	U_{33}	U_{12}	U_{13}	U_{23}
Al	6d	1	1/4	0	1/2	0.00752(9)	Al	0.0065(2)	0.0080(1)	U_{22}	0	0	0
Si	6c	1	1/4	1/2	0	0.00754(8)	Si	0.0060(1)	0.0083(1)	U_{22}	0	0	0
O1	24i	1	0.14311(8)	0.15289(8)	0.4577(1)	0.0165(2)	O1	0.0145(3)	0.0142(2)	0.0210(3)	0.0001(2)	0.0015(2)	0.0070(2)
Na1	8e	0.5	0.1951(2)	x	x	0.0277(5)	Na1	0.0278(4)	U_{11}	U_{11}	0.0043(5)	U_{12}	U_{12}
Na2	8e	0.5	0.2793(2)	x	x	0.0296(6)	Na2	0.0296(6)	U_{11}	U_{11}	0.0095(6)	U_{12}	U_{12}
C	2a	1	0	0	0	0.062(2)							
X ^b	24i	0.25	0.034(1)	-0.104(1)	0.103(1)	0.075(4)							

^a $U_{iso} = 1/3 \sum_i \sum_j U_{ij} a_i^* a_j^* (\mathbf{a}_i \cdot \mathbf{a}_j)$ for the anisotropically refined atoms Al, Si, O1, Na1, and Na2. U_{ij} 's are defined for $\exp[-2\pi^2(h^2 a^* U_{11} + 2hka^* b^* U_{12} + \dots)]$. ^b Treated as oxygen in the refinements, the statistical occupancy factor (0.25) was multiplied by the factor 0.916 in order to account for the mixed occupation with $1/3\text{C} + 2/3\text{O}$.

Table 4. $[\text{Na}_4(\text{HCOO})]_2[\text{Al}_3\text{Si}_3\text{O}_{12}]_2$ (2): Fractional Atomic Coordinates and Isotropic Displacement Parameters U_{iso} (\AA^2) for Structure Model ii

atom	Wyckoff position	occupancy factor	x	y	z	U_{iso}
Al	6d	1	1/4	0	1/2	0.0030(4)
Si	6c	1	1/4	1/2	0	U_{Al}
O1	24i	1	0.1400(3)	0.1503(3)	0.4437(3)	0.019(1)
Na	8e	1	0.1900(2)	x	x	0.053(1)
C	12f	0.1667	0.042(3)	0	0	0.15(5)
O2	24i	0.1667	-0.106(4)	-0.077(5)	0.021(5)	0.049(4)

Table 5. $[\text{Na}_5(\text{CO}_3)][\text{Na}_3\text{O}][\text{Al}_3\text{Si}_3\text{O}_{12}]_2$ (3): Fractional Atomic Coordinates and Isotropic Displacement Parameters U_{iso} (\AA^2)

atom	Wyckoff position	occupancy factor	x	y	z	U_{iso}
Al	6d	1	0.2438(9)	0	1/2	0.0054(4)
Si	6c	1	0.2530(9)	1/2	0	U_{Al}
O1	12j	1	0.1420(9)	0.1437(9)	0.4538(7)	0.014(1)
O2	12j	1	0.6530(9)	0.6401(9)	0.9570(7)	0.014(1)
Na1	4e	1	0.1859(4)	x	x	0.036(2)
Na2	4e	0.75	0.7275(7)	x	x	0.064(4)
Na3	4e	0.25	0.2083(9)	-x	-x	U_{Na2}
C	1a	1	0	0	0	0.07(1)
O3	12j	0.25	0.060(1)	-0.052(1)	0.111(1)	0.02 ^a

^a Parameter was kept fixed in refinement.

Table 6. $[\text{Na}_4(\text{CH}_3\text{COO})]_2[\text{Al}_3\text{Si}_3\text{O}_{12}]_2$ (1): Selected Interatomic Distances (\AA) and Angles (deg)

Host Structure			
Al-O1	1.736(1)	Si-O1	1.616(1)
O1-Al-O1 (4 \times)	108.19(3)	O1-Si-O1 (4 \times)	107.31(3)
O1-Al-O1 (2 \times)	112.06(6)	O1-Si-O1 (2 \times)	113.89(6)
Al-O1-Si	146.36(6)		
Sodium Coordination			
Na1-O1	2.460(2)	Na1-O1	2.950(1)
Na2-O1	2.338(1)	Na2-O1	3.062(2)
Na1-X	2.39(1)	Na2-X	2.27(1)
Acetate Anion			
C-X	1.38(2)		

Table 7. $[\text{Na}_4(\text{HCOO})]_2[\text{Al}_3\text{Si}_3\text{O}_{12}]_2$ (2): Selected Interatomic Distances (\AA) and Angles (deg)

Host Structure			
Al-O1	1.745(3)	Si-O1	1.622(3)
O1-Al-O1 (4 \times)	108.5(1)	O1-Si-O1 (4 \times)	107.6(1)
O1-Al-O1 (2 \times)	111.4(1)	O1-Si-O1 (2 \times)	113.4(1)
Al-O1-Si	140.4(2)		
Sodium Coordination			
Na-O1	2.343(1)	Na-O1	3.040(3)
Na-O2	2.27(4)	Na-O2	2.92(4)
Formate Anion			
C-O2	1.31(1)	O2-C-O2	128.4(6)

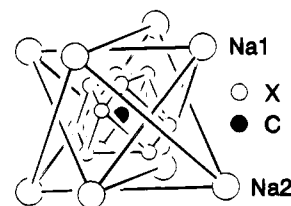
possessing attractive interactions with the negatively charged carboxylate group being modeled by Na1.

At room temperature the disorder of cations and anions is dynamical in nature as inferred from the ^{23}Na MAS NMR spectrum shown in Figure 4a. This spec-

Table 8. $[\text{Na}_5(\text{CO}_3)][\text{Na}_3\text{O}][\text{Al}_3\text{Si}_3\text{O}_{12}]_2$ (3): Selected Interatomic Distances (\AA) and Angles (deg)

Host Structure			
Al-O1	1.693(7)	Si-O1	1.617(9)
Al-O2	1.740(8)	Si-O2	1.620(7)
O1-Al-O1 (1 \times)	107.3(6)	O1-Si-O1 (1 \times)	113.0(5)
O1-Al-O2 (2 \times)	110.8(1)	O1-Si-O2 (2 \times)	107.8(1)
O1-Al-O2 (2 \times)	107.6(2)	O1-Si-O2 (2 \times)	109.2(2)
O2-Al-O2 (1 \times)	112.5(5)	O2-Si-O2 (1 \times)	109.6(6)
Al-O1-Si	145.9(3)	Al-O2-Si	147.3(3)
Sodium Coordination			
Na1-O1	2.481(2)	Na1-O2	2.971(4)
Na1-O3	2.522(2)	Na1-O3	2.620(2)
Na2-O1	2.976(4)	Na2-O2	2.348(3)
Na3-O1	3.196(4)	Na3-O2	2.40(1)
Na3-O3	2.05(1)		
Carbonate Anion			
C-O2	1.231(9)	O3-C-O3	120.0 ^a

^a Angle was constrained at 120 $^\circ$.

**Figure 3.** $[\text{Na}_4(\text{CH}_3\text{COO})]_2[\text{Al}_3\text{Si}_3\text{O}_{12}]_2$ (1): Time- and space-averaged positions of the guest atoms Na1, Na2, C(carboxylate), and X (weighted average of the oxygen and methyl carbon atoms).

trum exhibits only a single, slightly broadened line at -7.4 ppm. Additionally, the lineshape reveals that the electric-field gradient (EFG) at the quadrupolar ^{23}Na nuclei ($I(^{23}\text{Na}) = 3/2$) is dynamically averaged. A static-disorder would most probably lead to a more complex ^{23}Na MAS NMR spectrum.

Structure of Sodium Formate Sodalite (2). In the IR spectrum the characteristic $\nu(\text{C}-\text{O})$ vibrations of the carboxylate anion are seen at 1352 and 1613 cm^{-1} , which is in accordance with the frequencies measured for sodium formate (1364 and 1607 cm^{-1}).²⁰ Weak bands occur at 2670, 2770, and 2969 cm^{-1} . Thus the IR spectrum demonstrates that intact formate anions have been trapped in the sodalite cages during hydrothermal synthesis. In the ^1H MAS NMR spectrum the formyl proton causes a single sharp line at 8.8 ppm (298 K).

Structure model ii has been chosen as the best one out of the four models considered in the Rietveld analysis for reasons discussed above (see Crystal Structure Refinements). Each sodalite cage is occupied by

(20) Schrader, B., Meier, W., Eds., *IR Atlas of Organic Compounds*; Verlag-Chemie: Weinheim, 1977; spectrum B3-16.

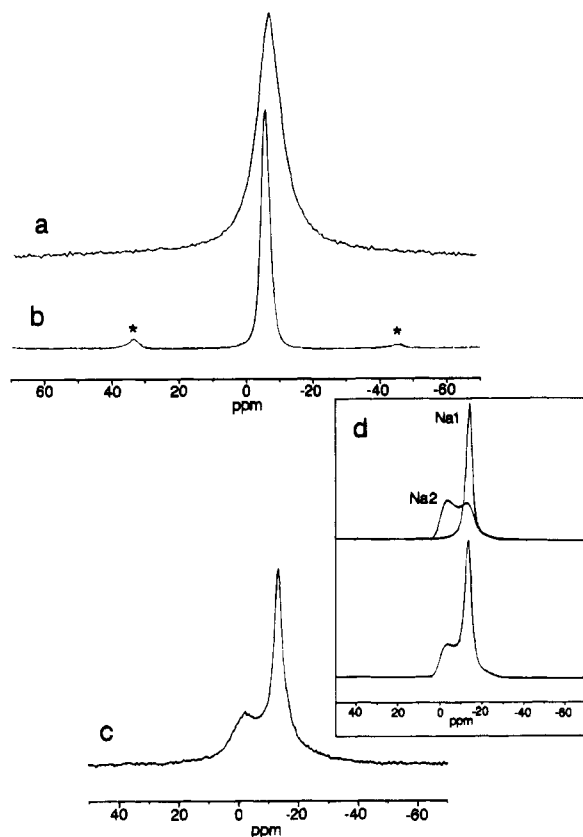


Figure 4. ^{23}Na MAS NMR spectra measured at 298 K for (a) $[\text{Na}_4(\text{CH}_3\text{COO})]_2[\text{Al}_3\text{Si}_3\text{O}_{12}]_2$ (**1**), (b) $[\text{Na}_4(\text{HCOO})]_2[\text{Al}_3\text{Si}_3\text{O}_{12}]_2$ (**2**), (c) $[\text{Na}_5(\text{CO}_3)][\text{Na}_3\Box][\text{Al}_3\text{Si}_3\text{O}_{12}]_2$ (**3**). In (d) the simulation of the spectrum of **3** (bottom) with the component signals A and B (top) is shown; the spectral parameters are as follows, component A QCC = 2.30 MHz, $\eta_Q = 0$, $\delta = 4.0$ ppm; component B QCC = 0 MHz, $\eta_Q = 0$, $\delta = -13.1$ ppm.

four ordered sodium cations Na on the 3-fold axes of the structure and by an orientationally disordered formate anion at the center. In the time- and space-averaged picture derived from X-ray diffraction, the oxygen atoms O2 of the anion form a polyhedron which can be described as a distorted icosahedron (Figure 5a). Within this icosahedron, the carbon atom C is located off-center in such a way that the 2-fold axis of the anion (symmetry $mm2/C_{2v}$) coincides with a 2-fold axis of the structure (Figure 5b). Owing to the high symmetry of the center of the sodalite cage (23), six different orientations occur for an anion. For one given orientation, two of the four sodium cations are coordinated by three framework oxygen atoms O1 at distances of 2.343(3) Å and by one O2 atom at a distance of 2.27(4) Å, while the remaining sodium cations are coordinated exclusively by O1 atoms.

It should be noted that the rather peculiar Na coordinations discussed above violate simple valence-bond arguments and that the disorder model has approximate character only. This is in line with the ^{23}Na MAS NMR spectrum which exhibits only a single narrow signal at -7.1 ppm (Figure 4b), revealing that at room temperature the four cations have the same environment on the time scale of the NMR experiment, i.e., the orientational disorder of the anion is dynamical in nature.

Due to the smaller size of a formyl proton as compared to a methyl group, the sodium cations experience weaker Na-H(anion) repulsive forces in **2** than in **1**,

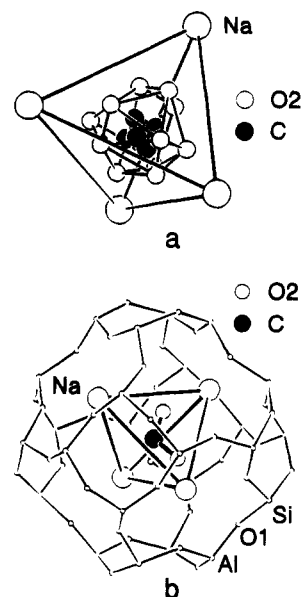
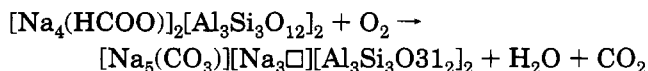
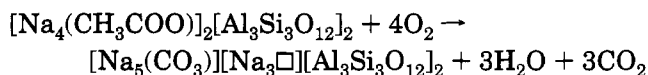


Figure 5. $[\text{Na}_4(\text{HCOO})]_2[\text{Al}_3\text{Si}_3\text{O}_{12}]_2$ (**2**): (a) Time- and space-averaged picture of the guest atoms, (b) sodalite cage with the guest species in one arrangement.

explaining why clear positional cation disorder is found only in the latter case. The structure of **2** may also be compared with the structure of sodium nitrite sodalite $[\text{Na}_4(\text{NO}_2)]_2[\text{Al}_3\text{Si}_3\text{O}_{12}]_2$,²¹ where the cations are also ordered. We presume that in **2** there occur besides strong attractive Na-O(anion) interactions also, yet weaker, attractive forces between the Na^+ cations and the C atom of the formate anion ($d(\text{Na}-\text{C}) = 2.75(2)$ Å). This would be in analogy to the situation in sodium nitrite sodalite, where attractive Na-N(nitrite) interactions clearly occur.²¹ The interaction Na-H(formate) in **2**, which is repulsive rather than attractive, might then be responsible for the larger cell constant of **2** ($a = 8.960$ Å) as compared with cubic sodium nitrite sodalite ($a = 8.923$ Å).²⁰

Thermogravimetric Studies on 1 and 2. The simultaneous thermal analysis (STA) curves of **1** and **2** measured in flowing oxygen are displayed in Figure 6. The weight losses in the TG traces reveal that the acetate and formate anions are oxidized to carbonate anions at approximately 1100 and 900 K, respectively, without destruction of the sodalite host framework, thus producing sodium carbonate sodalite $[\text{Na}_5(\text{CO}_3)][\text{Na}_3\Box][\text{Al}_3\text{Si}_3\text{O}_{12}]_2$ (**3**) according to the following reactions:



Simultaneous mass spectrometric analysis shows that volatile substances evolved from **1** and **2** during that oxidation reactions are H_2O , CO_2 , and small amounts of CO. The presence of CO indicates that oxidation of the trapped carboxylate anions is not complete with the heating rate (10 K min^{-1}) employed. Indeed, the final decomposition products of **1** and **2** (see below) were grey

(21) Sieger, P.; Wiebcke, M.; Felsche, J.; Buhl, J.-Ch. *Acta Crystallogr.* **1991**, C47, 498. Kempa, P. B.; Engelhardt, G.; Buhl, J.-Ch.; Felsche, J.; Harvey, S.; Baerlocher, Ch. *Zeolites* **1991**, 11, 558.

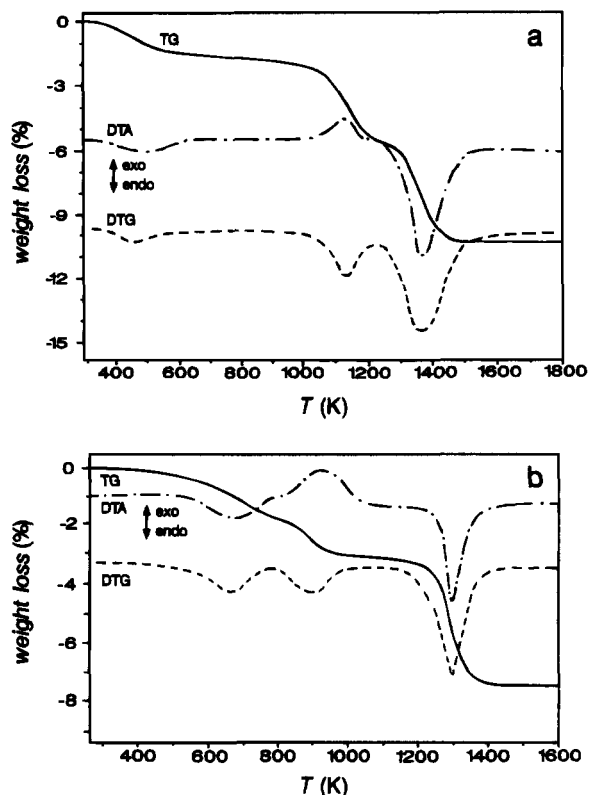


Figure 6. Simultaneous thermal analysis curves measured in flowing oxygen for (a) $[\text{Na}_4(\text{CH}_3\text{COO})_2]_2[\text{Al}_3\text{Si}_3\text{O}_{12}]_2$ (**1**) and (b) $[\text{Na}_4(\text{HCOO})_2]_2[\text{Al}_3\text{Si}_3\text{O}_{12}]_2$ (**2**).

or even black due to the presence of coke. However, slower heating rates ($<1 \text{ K min}^{-1}$) produced a white, fully oxidized material. Further decomposition of the (intermediate) phase **3**, accompanied by a destruction of the sodalite framework, takes place between 1250 and 1400 K, yielding as final product a stuffed derivative of carnegieite with the composition $\text{Na}_2\text{O} \cdot 6\text{NaAlSiO}_4$.²² It should be noted that single crystals of **1** crack during this thermal treatment.

On a larger scale, pure polycrystalline material of **3** has been obtained by annealing **1** (ground crystals) and **2** in air at temperatures of 1123 K (60 h) and 923 K (16 h), respectively. Long reaction times are needed because the "intracage" oxidation of **1** and **2** toward **3** is kinetically controlled; the rate-limiting factor is probably the diffusion of oxygen into and between the cages. The intracage oxidation is complete under such annealing conditions as proved by IR spectroscopy. In the spectrum of **3** the strong $\nu(\text{C}-\text{O})$ vibration band of the carbonate anion is observed at 1427 cm^{-1} (Na_2CO_3 : $\nu(\text{C}-\text{O}) = 1449 \text{ cm}^{-1}$ ²³), while no bands are seen in the ranges typical for the $\nu(\text{C}-\text{O})$ and $\nu(\text{C}-\text{H})$ vibrations of the carboxylate anions. Additionally, the ^{13}C MAS NMR spectrum of **3** exhibits a single sharp line with a chemical shift of 171.6 ppm which is close to the shift of 169.5 ppm observed for the CO_3^{2-} anion in aqueous solution.²⁴

Structure of Sodium Carbonate Sodalite (**3**).

From the Rietveld refinement in space group $P23$ the following structure model was obtained. The carbonate

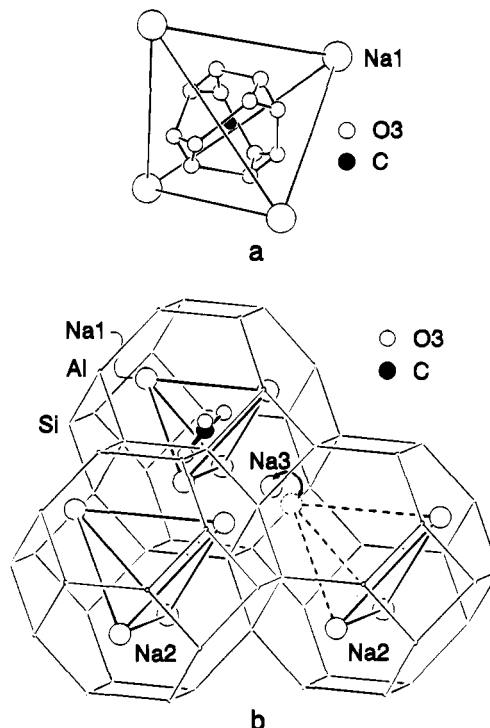


Figure 7. $[\text{Na}_5(\text{CO}_3)][\text{Na}_3\text{O}][\text{Al}_3\text{Si}_3\text{O}_{12}]_2$ (**3**): (a) Tetrahedron of Na1 cations with truncated tetrahedron formed on time and space average by the oxygen atoms O3 of the carbonate anion, (b) "snapshot" of one arrangement of guest species within the host framework represented by the tetrahedrally coordinated atoms (Al and Si) only; the double arrow points to two mutually exclusive positions of cation Na3 in adjacent cages.

anions center only every other sodalite cage, while the remaining cages are free of anions. The oxygen atoms O3 of a given anion are distributed statistically between 12 positions, thus forming on time and space average a truncated tetrahedron (Figure 7a). Three of the O3 atoms can be picked to generate a carbonate anion (symmetry $\bar{6}2m/D_{3h}$), the 3-fold axis of which coincides with a 3-fold axis of the structure. Again, orientational disorder is enforced because of the misfit of the symmetries of the anion and the center of the sodalite cage (23).

There occur three crystallographically distinct sodium cations, each being located on the 3-fold axes of the structure as is shown in Figure 7b. Four Na1 cations (occupancy factor 1.0) form a regular Na_4 tetrahedron around a carbonate anion. Each of these cations is coordinated by three framework oxygen atoms O1 at distances of $2.481(2) \text{ \AA}$. Depending on the orientation of the anion, three out of the four Na1 atoms are coordinated in addition by two oxygen atoms O3 of the anion at distances of $2.522(2) \text{ \AA}$. Four Na2 cations (occupancy factor 0.75) are located in each anion-free cage. These cations are each bonded to three framework oxygen atoms O2 at distances of $2.348(3) \text{ \AA}$. Finally, four Na3 cations (occupancy factor 0.25) appear in each anion-bearing cage. These cations are each coordinated by three framework atoms O2 at distances of $2.40(1) \text{ \AA}$. There is no further coordination of Na3 cations by oxygen atoms of the anion, since the $\text{Na3}-\text{O3}$ contacts are either too long ($\geq 3.40(1) \text{ \AA}$) or too short ($2.05(1) \text{ \AA}$), thus ruling out a simultaneous occupation of both the Na3 and the O3 position in the latter case. Instead, an

(22) Klingenberg, R.; Felsche, J. *J. Solid State Chem.* **1986**, *61*, 40.

(23) Ross, S. D.; Goldsmith, J. *Spectrochim. Acta* **1964**, *20*, 781.

(24) Abbott, T. M.; Buchanan, G. W.; Kruus, P.; Lee, K. C. *Can. J. Chem.* **1982**, *60*, 1000.

Na3 cation possibly interacts weakly with the whole π -electron system of the carbonate anion, as may also be the case for that Na1 cation opposite to the given Na3 cation in the same cage ($d(\text{Na1}\cdots\text{C}) = 2.91(1) \text{ \AA}$, $d(\text{Na3}\cdots\text{C}) = 3.26(1) \text{ \AA}$). In summary, the cages in **3** house either $[\text{Na}_5(\text{CO}_3)]^{3+}$ or $[\text{Na}_3\Box]^{3+}$ clusters. By these kinds of filling the inhomogeneous charge distribution from the three negative framework charges per sodalite cage and the two negative charges from the carbonate anion in every other cage are balanced locally in an optimum manner. A "snapshot" picture of a possible arrangement based on the given arguments is provided in Figure 7b.

The ^{23}Na MAS NMR spectrum of **3** is displayed in Figure 4c. Computer simulation of the spectrum revealed that it consists of two overlapping components (Figure 4d). One component (A) exhibits a typical quadrupolar line shape characterized by a quadrupole coupling constant (QCC) of 2.3 MHz, an asymmetry parameter of the electric field gradient (η_Q) close to zero, and an isotropic chemical shift (δ_{iso}) of 4.0 ppm. The other component (B) is a narrow Gaussian line at $\delta_{\text{iso}} = -13.1$ ppm, indicating no or only weak quadrupole interactions. Component A is assigned to the cations Na2 and Na3 which experience strong quadrupole interactions due to the electric field gradient induced by the one-sided but axially symmetrical coordination to three framework²⁵ O1 atoms. The appearance of only one signal for Na2 and Na3 indicates a fast (on the NMR time scale) dynamical exchange process between both cation sites in adjacent cages across the six-membered ring of the host framework ($d(\text{Na2}\cdots\text{Na3}) = 1.32(1) \text{ \AA}$), as marked by the double arrow in Figure 7b. Simultaneously with this site exchange process there occurs, most probably, a synchronized dynamical reorientation of the carbonate anion, as can be inferred from the too short Na3 \cdots O3 distance (2.05 \AA) discussed above. Component B of the ^{23}Na MAS NMR spectrum corresponds to the cations Na1 which show no or only weak quadrupole coupling since they reside on time-average in a

highly symmetrical oxygen coordination created by the fast rotational diffusion of the CO_3^{2-} anion and the similar Na1 \cdots O1 and Na1 \cdots O3 distances.

Conclusions

Our studies on organic anions containing sodalites provide important results with regard to weak and strong, attractive and repulsive, interactions between organic molecules and inorganic solid matter. This is seen for example in the comparison between the structures of **1** and **2**, where despite of the chemical similarity of the carboxylate anions the substitution of the formyl proton by the methyl group of the acetate anion induces disorder in the positions of the cations. In some cases, as described above, it is tempting to speculate about weak attractive interactions between the Na^+ cations and the π -electron systems of the anions. Another important aspect is the fact that the orientational disorder of the anions is dynamical already at room temperature. This is not the case in the pure sodium salts and clearly caused by the "matrix-isolated" state of the anions enclosed in the sodalite framework. These features are of interest for a better understanding of the interaction of organic molecules with inorganic solid matter in other fields such as heterogeneous catalysis, biomineralization, and biomimetic synthesis procedures. Our research on such model systems now focuses on the structure and dynamics of sodalites $[\text{M}]_2[\text{Si}_6\text{O}_{12}]_2$ with a pure silica framework enclathrating neutral organic molecules M. In these systems, host-guest interactions are restricted to van der Waals forces and (possibly in some cases) weak hydrogen bonds. Ionic interactions are excluded, however.

The high thermal stability of the periodic sodalite matrix enabled us to carry out a high-temperature intracage reaction to modify the guest species and to produce a sodalite not accessible by direct hydrothermal synthesis. The most interesting result in the case of this carbonate sodalite (**3**) is the answer to the question how the system, spatially organized by the sodalite framework, reacts to an uneven distribution of the negative charges of the anions: It increases the positional disorder of the cations, so that the distribution of positive charges becomes uneven just as well. This uneven distribution of positive and negative charges may well be a reason for the obstruction of the direct synthesis path.

(25) Engelhardt, G.; Sieger, P.; Felsche, J. *Anal. Chim. Acta* **1993**, *283*, 967.

(26) Sheldrick, G. M. *SHELXL-93*, Universität Göttingen, 1993.

(27) *International Tables for Crystallography*; Kluwer Academic Publishers: Dordrecht, Holland, Vol. C, 1992; pp 193, 219, 500.

(28) Baerlocher, Ch. *The X-ray Rietveld System*, Version of Sept 1982, ETH, Zürich.

(29) *International Tables for X-ray Crystallography*, Kynoch Press: Birmingham, 1974; Vol. IV, pp 99, 149.